5.5 Overmixing and maximal flow in estuaries.

As discussed in the previous section, two-layer exchange flows exhibit a range of critically controlled steady states. Given certain restraints imposed by the upstream conditions, there generally exists a family of 'submaximal' solutions in which one of the layers acts more or less like a single-layer (reduced-gravity) flow while the other layer remains relatively passive. There is a single section of critical flow and the wave that is arrested is the one that attempts to propagate in the upstream direction of the 'active' layer. For a pure sill geometry, only the lower layer can be the relatively 'active' one. For a pure contraction, either layer may be the relatively active one. There is also a particular solution that is characterized by the presence of two critical sections and is a limiting case of the above solutions. One control often acts where the upper layer is active while the other acts where the lower layer is active. Such controls arrest wave propagation opposite to the direction of flow in the active layer. In the example of flow from a deep basin over a pure sill, the 'lower layer control' lies at the sill while the 'upper layer control' lies in one of the neighboring basins. In the case of a pure contraction with pure exchange, both critical states coincide at the narrowest section and both layers are active. The theory for these idealized geometries has been extended to include situations where the sill and narrowest width occur at different sections. Farmer and Armi (1986) have shown that the maximal solution in this case has one control section at the narrows and the second at the sill.

For a steady exchange flow with fixed reduced gravity g' and flux ratio Q_r the solution with two critical sections has maximal exchange transport. The control sections for the maximal solution are insulated from the far field by stretches of supercritical flow that extend into the reservoir, terminating in hydraulic jumps. Linear wave propagation is permitted into, but not out of, the end basins. In this way, the flow at the control sections (particularly the exchange transport) is immune to mechanical changes that occur in the end basins. For example, a slight changed in the interface level that is forced in one of the basins will generate an internal wave that will spread over the basin, but not into the strait. At the same time, changes in material properties such as density, which are advected by the flow, are not restricted in the same way. A forced change in layer density, and thus g', in an upstream basin, will be carried through the strait regardless of the state of hydraulic criticality. The value of g' ultimately depends on how the flow is forced and how the two layers are mixed.

Although Long's (1954) experiments, their descendants, and other initial-value experiments are helpful in developing intuition about maximal and submaximal flows, it is usually difficult to extrapolate the results to particular geophysical settings. For example, oceanographically relevant exchange flows often originate from an upstream basin or estuary that has finite extent and is subject to forcing, dissipation and mixing. The upstream conditions are therefore quite different from those envisioned by Long. Usual forcing mechanisms include cooling, evaporation, and precipitation over the basin surface, inflows and outflows from other straits or rivers, and mechanical forcing due to winds and tides. Estuaries are fed by a source of fresh runoff water that floats above the denser, saline ocean water and flows out into the ocean proper. Turbulence generated by tides, winds and internal instabilities can lead to mixing of the two water masses and an increased salinity of the upper layer. The export of salt that occurs where the upper layer exits must be balanced by an inflow if deeper, saltier water, and an exchange flow is set up. Semi-enclosed seas having stong evaporation or cooling can act as ‘inverse estuaries’, where the exchange flow is reversed. Two of the most widely studied examples are the Red Sea and Mediterranean Sea, which experience excessive evaporation and relatively little fresh water input from rivers. The combination of evaporation and surface cooling causes the surface waters to sink and eventually flow out into the ocean proper through the connecting passages, here the Bab al Mandab and the Strait of Gibraltar. Relatively fresh water is drawn in at the surface of these straits, resulting in exchange flows. Whether the latter are maximal or submaximal is a question that has excited a great deal of debate.

Under conditions of steady flow in a closed basin with observable air-sea fluxes it is easy to write down a number of constraints on the overall exchange flow. For example, the net volume transport out of the basin must be balanced by river runoff, precipitation, and evaporation:

$$\iint_{A_s} (E-P)dA = -(Q_R{*} + Q_1{*} + Q_2{*}) \qquad (5.5.1)$$

where E-P represents the volume flux per unit surface area due to evaporation minus precipitation, A_s is the surface area of the basin, and $-Q_R{*}$ is the volume inflow due to river runoff. If there are differences in the concentration of a chemical tracer between the inflow and outflow and if the sources and sinks of this tracer in the basin can be quantified, then a similar conservation law can be written down. For example, the input of salt due to river runoff in the Red Sea and Mediterranean Sea is negligible and thus the total influx of salt must be approximately zero:

$$Q_1{*}S_1 + Q_2{*}S_2 = 0. \qquad (5.5.2)$$

Equations (5.5.1) and (5.5.2) can be rearranged to yield Knudsen’s relations

$$Q_1{*} = \frac{S_2\left[\iint_{A_s} (E-P)dA + Q_R{*}\right]}{S_1 - S_2} \qquad (5.5.3a)$$

and

$$Q_2{*} = \frac{S_1\left[\iint_{A_s} (E-P)dA + Q_R{*}\right]}{S_2 - S_1}, \qquad (5.5.3b)$$

named after Danish chemist and oceanographer. The salinity of the inflowing layer (either S_1 or S_2) is equal to the salinity of the ocean water that is drawn in and can nominally be regarded as known. We will also assume that the values of E-P and Q_R* are known, even though the uncertainties in the measurement of these fluxes may be significant. If the salinity of the outflowing layer can be measured, then (5.5.3) can be used to calculate Q_1* and Q_2*.

The above approach appears was used by Neilsen (1912) to estimate the volume fluxes in the Strait of Gibraltar. Although they may provide a practical means for estimating layer fluxes, equations (5.5.3a,b) beg the question of what determines the salinity of the outflowing layer (or, equivalently, S_2-S_1). A theory that provides an answer is based on the idea of *overmixing*, first proposed by Stommel and Farmer (1953). Their ideas were formulated in the context of an estuarine circulation, where E-P is neglected, S_2 is regarded as fixed, and mixing between the upper and lower layers in the estuary interior is regarded as imposed independently of the mean circulation itself. One may begin by imagining an unmixed state in which the river discharge Q_R* produces a fresh layer of water (S_1=0) that passes through the surface of the estuary and exits at the mouth. If mixing with the lower saline layer is initiated, perhaps as a result of winds or tides, S_1 is increased and S_2-S_1 is decreased. Equations (5.5.3a,b) then show that Q_1* and Q_2* increase: the estuary acquires a weak inflow of salty ocean water and an increased outflow of brackish surface water. If the mixing is increased further, the salinity difference between the layers continues to decrease and a stronger exchange circulation is induced. This process may not, however, continue unabated. Eventually the exchange at the mouth of the estuary must reach a maximal value permitted by hydraulic constraints and mixing beyond this threshold should have no further effect.

These ideas can be cast in quantitative form by requiring that the flow at the mouth of the estuary be hydraulically controlled, even when the exchange flow is weak. Then

$$\frac{v_{1c}{*}^2}{g'd_{1c}*}+\frac{v_{2c}{*}^2}{g'd_{2c}*}=\frac{Q_1{*}^2}{g'w{*}_m^2\,d{*}_{1c}^3}+\frac{Q_2{*}^2}{g'w{*}_m^2\,d{*}_{2c}^3}=1\,, \qquad (5.5.4)$$

where the subscript 'c' refers to the quantities measured at the mouth. For the time being, we will assume that the mouth consists of a pure contraction, with minimum width w_m*, and with no sill or other topographic variation.

The density difference between the two layers is due primarily to the salinity difference and thus

$$\rho_2-\rho_1=\beta(S_2-S_1)$$

where β ($=0.77\times10^{-3}$g cm^{-3} ppt^{-1}) is the coefficient of expansion of water due to salinity. In terms of the reduced gravity:

$$g' = g\frac{\beta(S_2 - S_1)}{\rho_o}. \tag{5.5.5}$$

If the depth at the mouth of the estuary is D_s, then $d_{1c}{}^* + d_{2c}{}^* = D_s$ or

$$d_{1c} + d_{2c} = 1 \tag{5.5.6}$$

where $d_{nc}=d_{nc}{}^*/D_s$.

Substitution of the (5.5.3) layer transports into (5.5.4) leads to

$$\frac{S_2^2}{d_{1c}^3} + \frac{S_1^2}{(1-d_{1c})^3} = \frac{g\beta w{*}_m^2\, D_s{}^3(S_2 - S_1)^3}{\rho_o Q_R{}^{*2}} \tag{5.5.7}$$

after use of (5.5.5) and (5.5.6). Further discussion of this relation can be simplified if it is assumed that $(S_2 - S_1)/S_2 << 1$, implying that $Q_1{}^* \cong -Q_2{}^*$ and therefore $Q_R{}^* << Q_1{}^*$. With this simplification, (5.5.7) can be written as

$$\frac{1}{d_{1c}^3} + \frac{1}{(1-d_{1c})^3} = (\Delta s)^3, \tag{5.5.8}$$

where

$$(\Delta s)^3 = \frac{g\beta w{*}_m^2\, D_s{}^3(S_2 - S_1)^3}{\rho_o Q_R{}^{*2}\, S_2^2}. \tag{5.5.9}$$

The relationship between the nondimensional salinity difference Δs and d_{1c} takes the form of a curve with two vertical branches and single minimum (Figure 5.5.1). For a given value of the nondimensional salinity difference Δs, and provided $(\Delta s)^3 > 16$, there are two roots d_{1a} and d_{1b}. Let us assume for the time being that the left branch of the curve gives the appropriate root. Begin at the state $d_{1c}=d_{1a}$ and imagine that the mixing increases while $Q_R{}^*$ is held fixed. Then S_2-S_1 should decrease, lowering the value of Δs, and the solution for d_{1c} is found by descent along the left branch of the solution curve. The minimum possible value of Δs lies at the base of the curve, where $d_{1c}=1/2$. The corresponding salinity difference

$$(S_2 - S_1) = \left(\frac{16\rho_o Q_R{}^{*2}\, S_2^2}{g\beta w{*}_m^2\, D_s{}^3}\right)^{1/3} \tag{5.5.8}$$

is the minimum possible, corresponding to the largest Q_1*(=-Q_2*), for the estuary. A further increase in the intensity of mixing in the estuary can apparently not alter these values and the resulting state is therefore 'overmixed'. It is not clear what this term implies for the interior state of the estuary itself, but some clues are provided by laboratory experiments to be presented here and in the next section. The analysis can also be carried out using the unapproximated version (5.5.7) of the governing relation and this leads to a skewed version of the Figure 5.5.1 curve (see Exercise 1).

In the overmixed limit, the interface depth at the estuary mouth lies at mid-depth and this corresponds to a state of maximal hydraulic exchange for flow through a pure contraction, as discussed in Section 5.4. Thus the state represented by the minimum of the Figure 5.5.1 curve represents a dynamically consistent state of maximal exchange in which the mouth, where the flow is critical, is insulated from both the ocean *and* the estuary by finite regions of supercritical flow. Other solutions lying along the left branch of the curve are hydraulically controlled, but submaximal. In these cases, supercritical flow exists only outside the estuary mouth.

The situation in which the mouth contains a sill is another matter. Let z_T* represent the depth, taken as constant, in the estuary interior, so that D_s/z_T*<1 when the mouth contains a sill. As discussed in Section 5.3, the corresponding maximal exchange solutions have unequal layer depths over the sill. When the sill is very shallow (D_s/z_T*<<1), d_1=0.625 and d_2=0.375 so that the interface lies below mid-depth. As the sill height D_s/z_T* is reduced, the interface rises eventually to mid-depth. The corresponding range of d_1 values is indicated by the solid segment of the curve in Figure 5.5.1. The limiting state of maximal exchange, and thus overmixing, in the presence of a sill therefore lies above the bottom of the curve and on the right branch. For a submaximal flow the interface at the sill lies below its level for maximal exchange. The corresponding 'undermixed' states lie along the right-hand branch of the curve. For these states supercritical flow extends from the mouth some distance *into* the estuary. If no sill is present, the choice between left and right branches depends on how the flow is established; the laboratory experiment described next selects the left branch.

The Stommel-Farmer hypothesis of an approach towards maximal estuary exchange and overmixing under conditions of controlled mixing has been investigated in a number of the laboratory experiments. Similar experiments geared towards inverse estuaries will be discussed in the next section. One method of controlling the mixing rate is to introduce fresh water into a salty laboratory estuary in the form of a turbulent plume of adjustable depth, and hence variable mixing. In Timmermans (1997), a small basin representing an estuary is connected to a salt-water reservoir by a narrows (Figure 5.5.2). The estuary receives a steady flux of fresh water through a small submerged tube at adjustable depth. The fresh influx forms an ascending turbulent plume that entrains salty water as it rises to the surface. Brackish plume water accumulates at the surface and exits horizontally through the narrows while salty water enters beneath to supply salt to the plume. As the depth over which the plume rises increases, so does the total amount of entrainment. The net upstream mixing in the experiment, thought by Stommel and

Farmer to be controlled by the tides or winds, can therefore be varied by injecting the fresh water at different depths.

Suppose that the plume is fed at elevation z_S* and volume rate Q_R* and that it ascends a height z_T*-d_u*- z_S* in order to the reach the base of the upper layer (Figure 5.5.2). The entrainment into the plume, and the corresponding value of g' at its top, can be estimated (Turner, 1973) using a theory for a self-similar plume rising through a quiescent fluid. The theory, which is based on the assumption that the source is weak (Q_R*<<Q_2*) yields

$$g' = 8.33\left[\left(g\beta S_2 Q_R *\right)^2 \left(z_T * - d_u * - z_S *\right)^{-5}\right]^{1/3}, \qquad (5.5.9)$$

where the leading coefficient is determined empirically.

This information may be used to predict the state of the exchange flow as a function of the source elevation z_S*. To do so, one must equate the internal energy (Bernoulli function) in the basin near the source to that at the narrowest section. If the approximation of zero net exchange is made, it follows that

$$\left\{\frac{1}{d_{1c}^2} - \frac{1}{\left(1-d_{1c}\right)^2}\right\} = \frac{2g\beta w^{*2}\, D_p^3 \left(S_2 - S_1\right)^3}{S_2^2 Q_R^{*2}}\left(d_{1c} - d_u\right) \qquad (5.5.10)$$

where d_{1c} and d_u are the upper layer depths at and upstream of the sill, nondimensionalized by the total depth D_s.

Equations (5.5.8-10) can be used to calculate the state variables (g', d_u, d_{1c}, etc.) as functions of the mixing parameter, z_S*, or equivalently d_S=(z_T*- z_S*)/D_S. For a given d_S, the exact location along the curve of possible solutions (Figure 5.5.1) can be found. Timmermans (1999) verified that increasing z_R, caused by a decrease in the source elevation, causes the solution to tend towards the overmixed limit and that data track the predicted curve quite well (Figure 5.5.3). However, even when the plume source is positioned at the bottom of the tank (d_S =1) the total entrainment is insufficient to reach the limit of overmixing, here the minimum of the curve. (The threshold d_S predicted by the theory is about 2.5.) This limitation can be overcome by adding more plumes and the 'x' symbols, representing experiments with 6 plumes, reach the threshold of overmixing.

One of the great mysteries raised by the hypothesis of overmixing concerns the state of the flow that occurs when this limit is exceeded. The basic premise is that the salinity difference between the two layers decreases as mixing increases, and that the exchange flow must increase to satisfy the overall salt budget. But what then happens when the exchange reaches its maximal value? A further increase in mixing would seem to require a further decrease in the salinity difference, leading to a violation of the salt budget. What happens under these conditions is not generally understood and undoubtedly depends on the way the flow is set up. The laboratory experiments described below and in the next section provide some insight.

Using an inverted version of the experiment described above, Whitehead et al. (2003) attempted to exceed the overmixed condition with a single plume and to provide some insight into the corresponding upstream state. The reservoir now contains fresh water and salt water is pumped in through a tube elevated above the bottom the 'estuary' basin (Figure 5.5.4). The full-depth narrows of the previous experiment is replaced with a submerged and shallower passage, similar to an upright experiment with a shallow sill. The mixing parameter d_S is now replaced by z_R ($=z_R^*/D_s$) the dimensionless source elevation above the bottom of the narrows. The new configuration allows a wider range of forcing.

The dyed salt plume appears on the far right in a photo (Figure 5.5.5). The salt-water layer appears black in the right basin and grey in the narrows because the basin is wider. The run shown is thought to exceed the limit of overmixing. The fresh upper layer flows into the basin from left to right and accelerates as it passes through the narrowest section and into the right basin. In the classical view, this flow would develop a hydraulic jump somewhere near the entrance to the basin. However, the region where this jump is expected shows billows (Figure 5.5.6). The latter cause the clear, fresh water entering the chamber to mix with the salty water, resulting in a brackish (grey) layer that extends into the basin up to the level of the tube source. The presumed maximal exchange flow should also have a hydraulic jump at the left end of the channel, and while this feature may have been present, it was not documented.

The approach to and beyond the limit of overmixing can been seen in a set of density profiles taken in the right basin (Figure 5.5.7). The value of z_R, now the elevation of the plume source, is labeled with each profile. The profiles show something like two homogeneous layers, often separated by a stratified, intermediate layer. The value of g' is defined using the difference between the local density and the density of the fresh water in the left reservoir. For the Stommel and Farmer theory, the relevant value of g' is based on the density difference between the upper and lower layers, measured at the narrowest section. This value is very close to the g' measured within the bottom layer of the profiles shown in the figures. It can be seen that as z_R is increased (the source is raised) from 1.5 to 2.5, the bottom value of g' decreases. Further increases in z_R cause g' to cluster around a value 0.105, though there is an unexplained minimum at z_R=3.0. Although the theoretical value g'=0.082 for this experiment is not reached, the convergence for values z_R>2.5 suggests that the exchange flow is close to or has exceeded the limit of overmixing. The theoretical underestimate may be due to the presence of frictional effects that have not been taken into account.

We now return to the conceptual question, raised earlier, regarding how the 'overmixed' flow conspires to keep g' at a relatively fixed value while the elevation of the plume source, and presumably the mixing, increases. An answer is suggested by two changes in the density distribution of the basin flow. One is a deepening of the lower layer and the other is the increased salinity of the overlying fluid (as evidenced by an increase in overall density). This second effect is due to the billows and other interfacial instabilities in and around the narrows, which cause the salty bottom layer to become entrained in the fresh layer entering from the reservoir. Now the total amount of salt in the estuary basin must remain constant, and thus the source salt flux must equal the salt flux through the narrows into the right reservoir. When the basin flow is undermixed, freshwater from the reservoir enters the basin and becomes entrained into the salty plume. As the plume mixing is increased and more fresh water is entrained, the plume is increasingly diluted, the density difference between layers decreases, and the exchange flow through the narrows intensifies. Once maximal exchange conditions in the narrows are reached, the amount of fresh water that can be drawn in from the reservoir cannot be increased. If one then attempts to increase the mixing further (by raising the source),the system responds in a way that limits the entrainment of fresh water. It does so by increasing the depth of the lower layer (thus limiting the vertical height over which mixing can occur) and by creating a mechanism by which salt is detrained into the incoming fresh water (thus increasing the salinity of the water that is entrained into the plume). In this respect the term 'overmixing' is misleading. Although the overall level of turbulence in the basin may increase, the actual net mixing between the fresh and salty layers remains fixed.

The overmixing hypothesis is by no means the only model of estuary dynamics. In fact, it is difficult to find examples of estuaries that clearly have maximal exchange at the mouth. The presence of strong time-dependence due to tides can cloud the interpretation. A reader interested in digging deeper into this field can consult Hetland and Geyer (2004), references contained therein, and also the textbook of Dyer (1997).

We end this section with a bit of speculation that some readers may wish to turn into careful research. The Black Sea acts like a giant estuary, with a relatively fresh surface layer fed by rivers and precipitation, and a deep, saline bottom layer. The Sea is connected to the Mediterranean by the Bosphorus, which contains a two-layer flow that exchanges fresh surface water for saline Mediterranean water. The lower layer of Mediterranean water begins its journey at a salinity of about 38 psu, passes through the Bosphorus, and descends in a turbulent plume into the Black Sea. Entrainment with the fresher (17 psu) water leads to dilution of this plume. The resulting water mass (about 22 psu) spreads throughout the deep Black Sea basin. The deep and shallow layers are separated by a pycnocline with a base at about 150m depth, well below the 40m deep Bosphorus.

There are two features that suggest that the Black Sea could be overmixed. One is the relatively deep pycnocline, similar to that in the inverted experiment (Figure 5.5.7). In that experiment, the interface or pycnocline in the right basin is much shallower than the passage. The second suggestive piece of evidence is that multiple sections of critical flow have been observed in the Bosphorus (Gregg and Özsoy, 2002), which could be consistent with maximal exchange.

Exercises

1) By rearranging the primitive version (5.5.7) of the relation governing estuary flow, show that

$$\frac{1}{d_{1c}^3}+\frac{(1-\tilde{\Delta}s)^2}{(1-d_{1c})^3}=\gamma(\tilde{\Delta}s)^3,$$

where $\tilde{\Delta}s=(S_2-S_1)/S_2$ and $\gamma=g\beta w_m D_s{}^3 S_2/\rho_o Q_R{}^{*2}$. For a (positive) γ of your choice, sketch the curve of $\tilde{\Delta}s$ vs. d_{1c} over $0<d_{1c}<1$ and note that the result is an asymmetrical version of the Figure 5.5.1 curve. Show that the minimum value of $\tilde{\Delta}s$ lies where

$$\frac{1}{d_{1c}^2}=\frac{(1-\tilde{\Delta}s)}{(1-d_{1c})^2}.$$

Deduce that this minimum must occur in $1/2\le d_{1c}<1$ and thus the interface must, in the overmixed limit, lie below mid-depth. Note that the minimum value of $\tilde{\Delta}s$ itself can be obtained by eliminating d_1 between the last two equations and solving the resulting polynomial.

2. How would the original theory of Stommel and Farmer be modified to fit the experimental conditions suggested in Figure 5.5.4?

Figure Captions

Figure 5.5.1. The dimensionless salinity difference Δs as a function of the dimensionless upper layer thickness d_{1c} at the mouth of an estuary, according to equation (5.5.8). The thickened portion of the curve shows the location of maximal exchange for a range of sill heights.

Figure 5.5.2 Sketch of the laboratory reservoir, fresh water source, and passage used to simulate an estuarine flow with partial mixing. The arrows indicate directions of flow.

Figure 5.5.3. The curve shows the predicted value of g' as a function of the dimensionless, critical upper layer depth d_{1c} at the narrowest section. The hash marks on the curve indicate where a solution with the indicated value of d_S should lie. The symbols indicate data points from the experiment of Timmermans (1999). Points indicate forcing by a single plume while crosses indicate six plumes.

Figure 5.5.4 Sketch of the Whitehead et al. (2003) laboratory setup.

Figure 5.5.5 Photograph of an experiment with z_R=3, thought to be overmixed.

Figure 5.5.6 Close-up of the flared region between the passage and the right basin where clear water flows up and into the chamber with developing billows. The experiment is the same as shown in Figure 5.5.6.

Figure 5.5.7 Density profiles for 14 experiments, measured at the location shown in Figure 5.5.4.

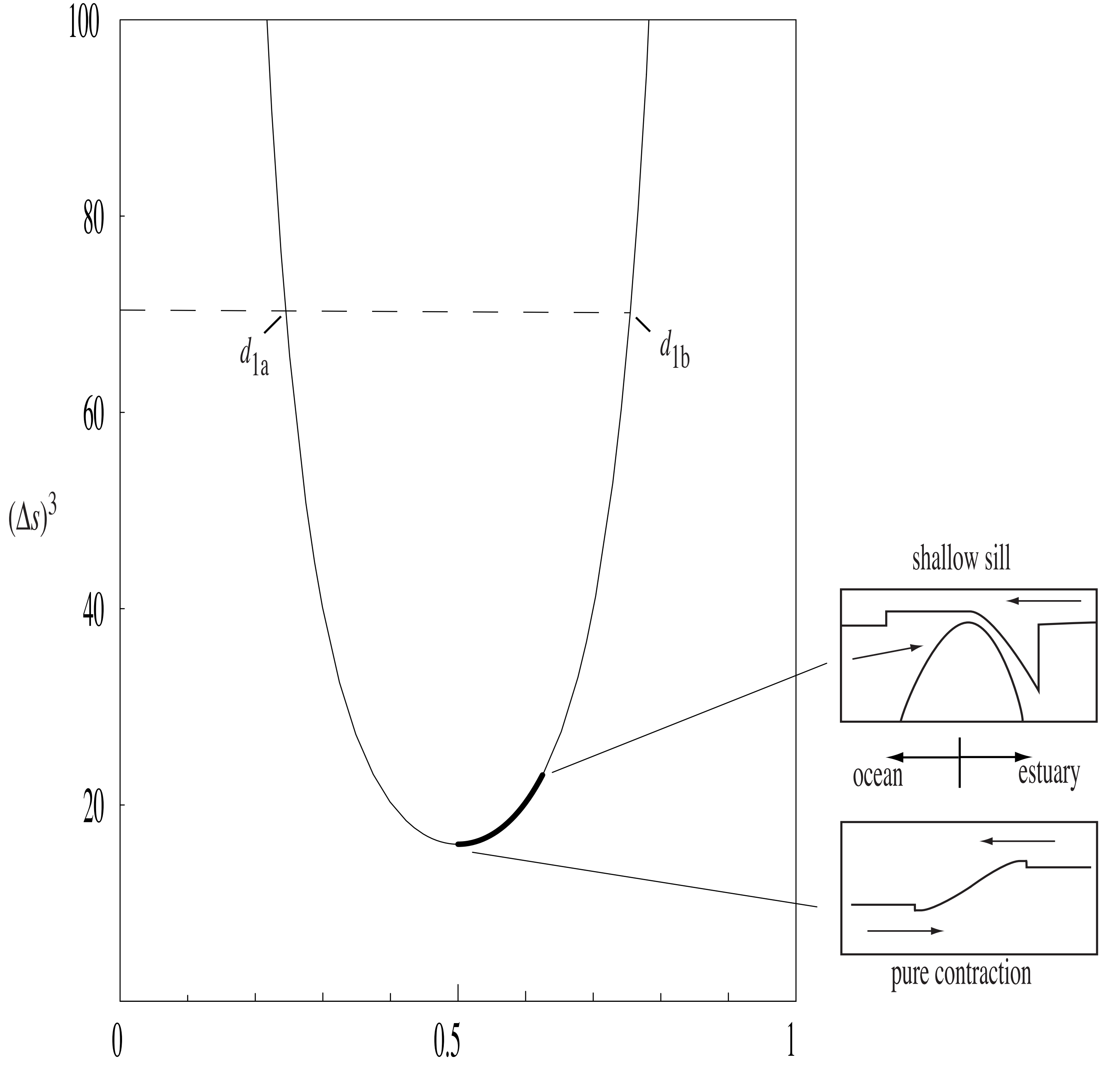

100
80
60
40
20
0
0.5
1
$(\Delta s)^3$
d_{1c}
d_{1a}
d_{1b}
shallow sill
ocean
estuary
pure contraction

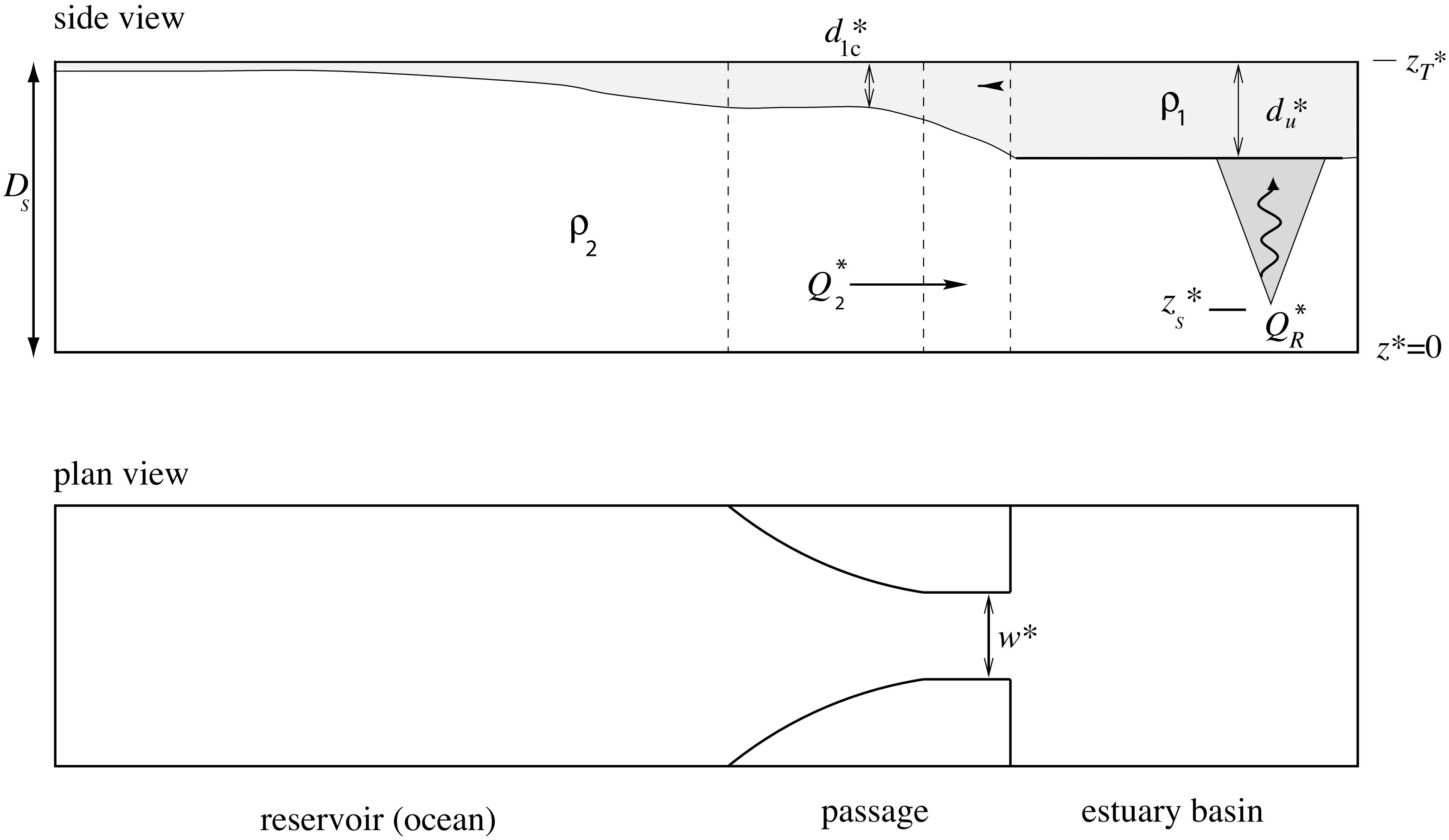
side view
d_{1c}^*
z_T^*
ρ_1
d_u^*
D_s
ρ_2
Q_2^*
z_s^*
Q_R^*
$z^*=0$
plan view
w^*
reservoir (ocean)
passage
estuary basin

Figure 5.5.2

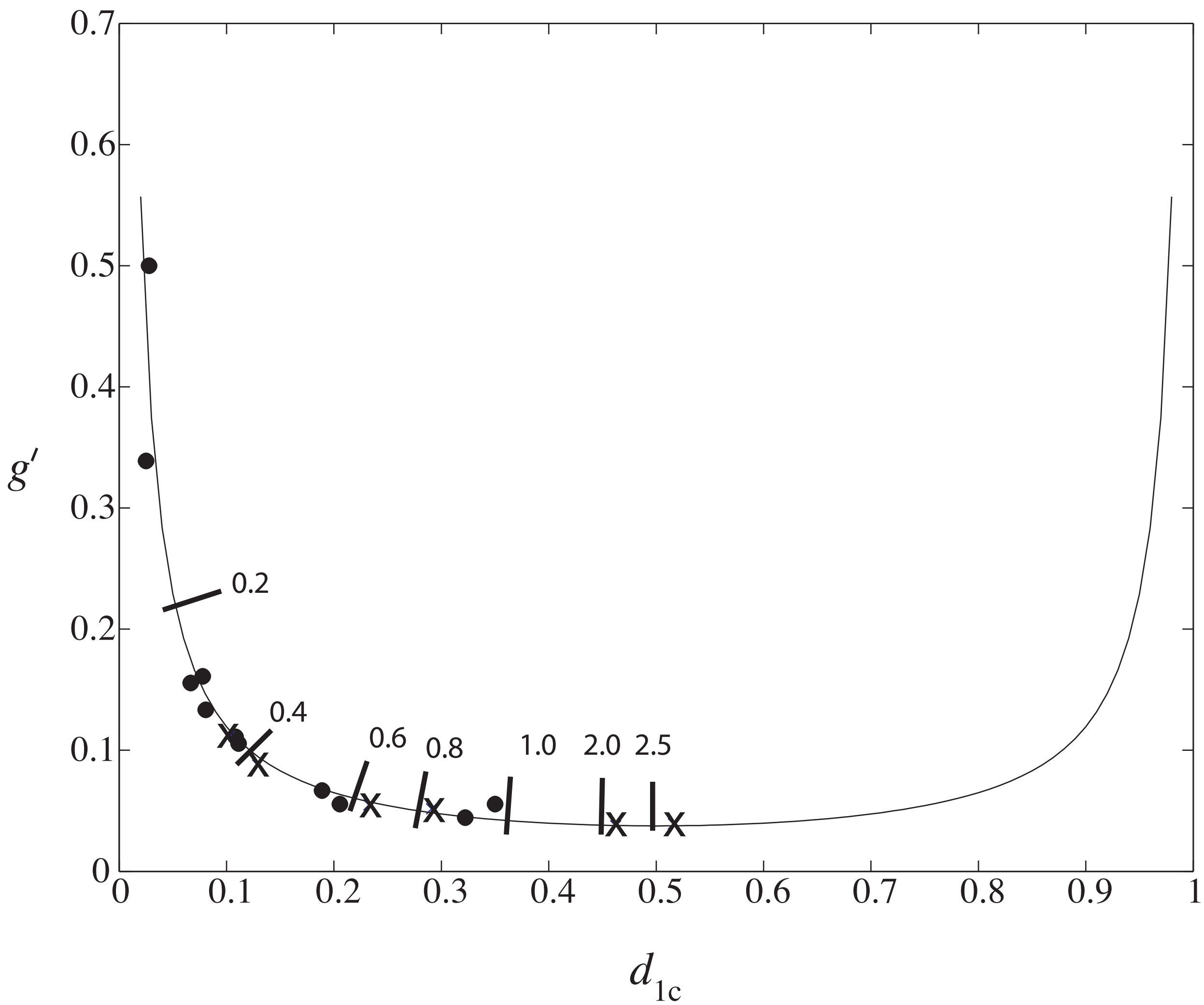

0.7
0.6
0.5
0.4
0.3
0.2
0.1
0
0
0.1
0.2
0.3
0.4
0.5
0.6
0.7
0.8
0.9
1
g′
d1c
0.2
0.4
0.6
0.8
1.0
2.0
2.5

Figure 5.5.3

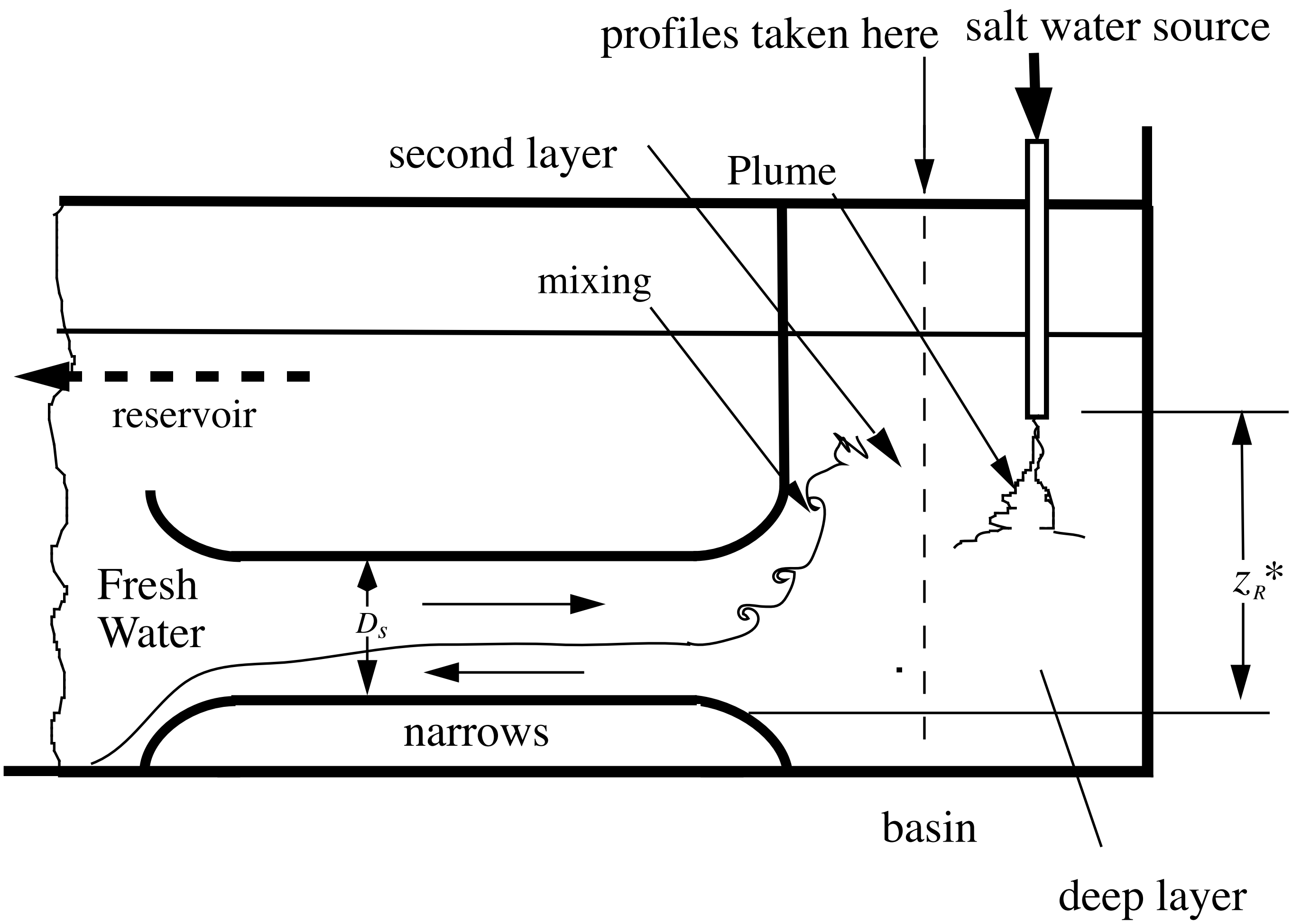

profiles taken here
salt water source
second layer
Plume
mixing
reservoir
Fresh
Water
D_S
z_R*
narrows
basin
deep layer

Figure 5.5.4

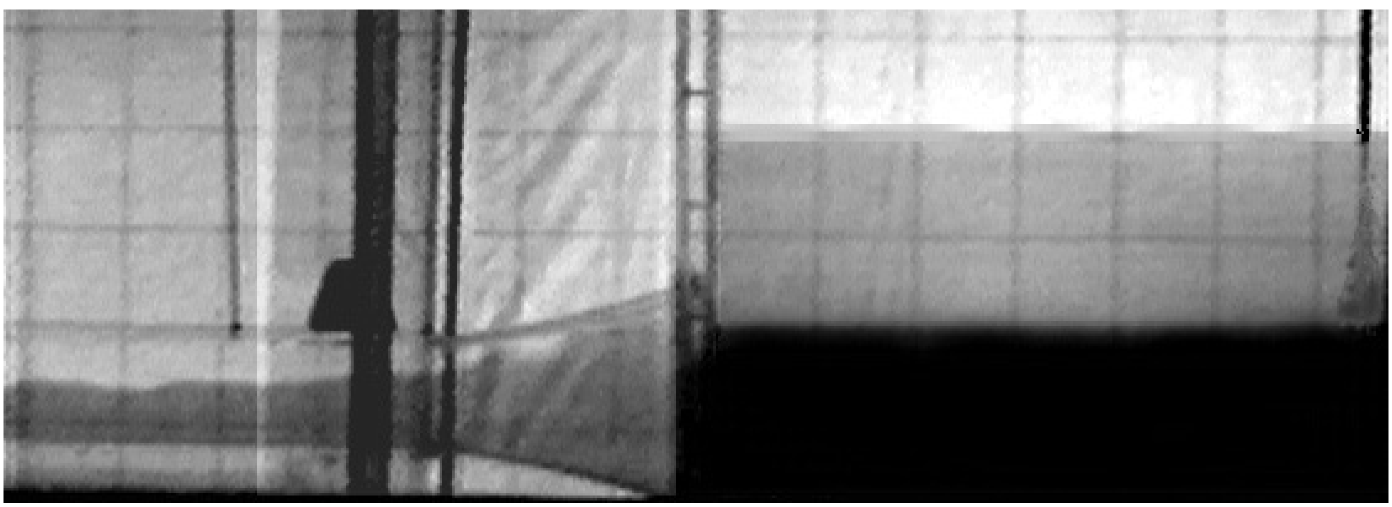

Figure 5.5.5

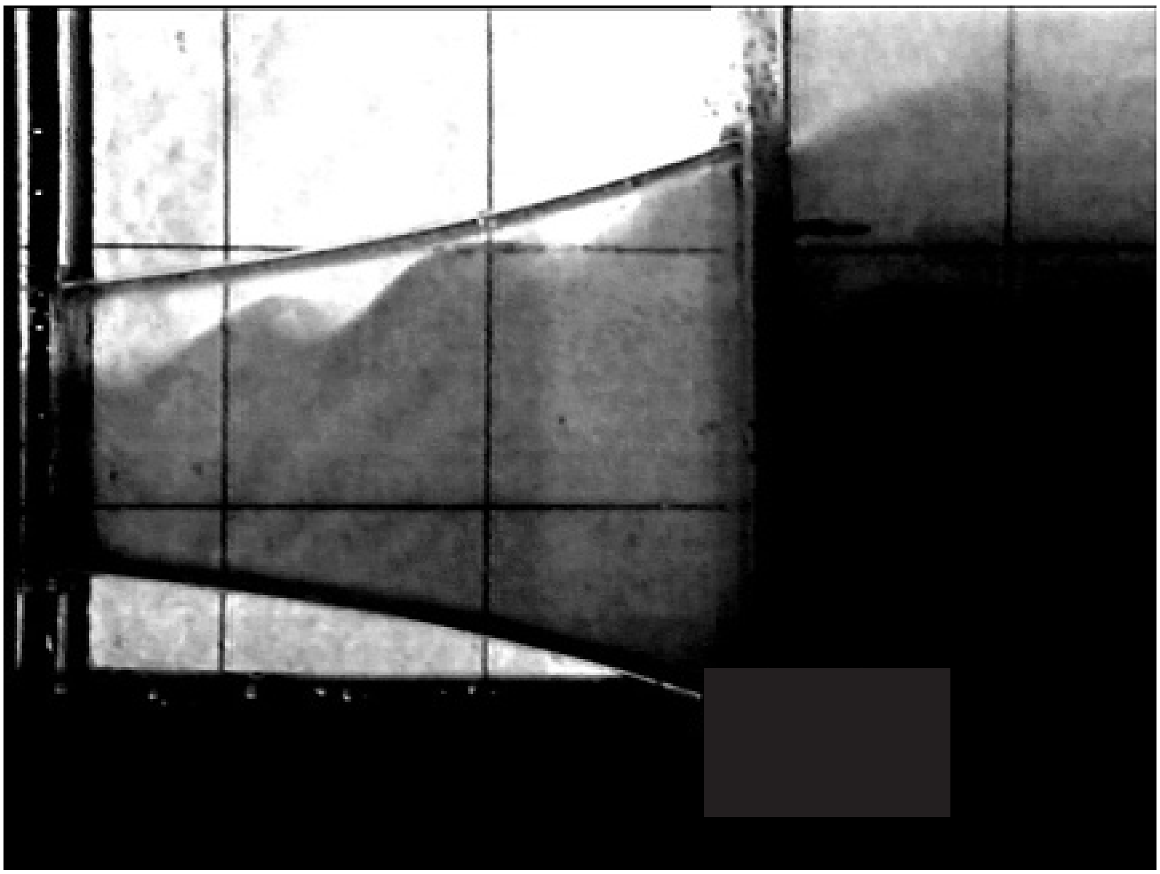

Figure 5.5.6

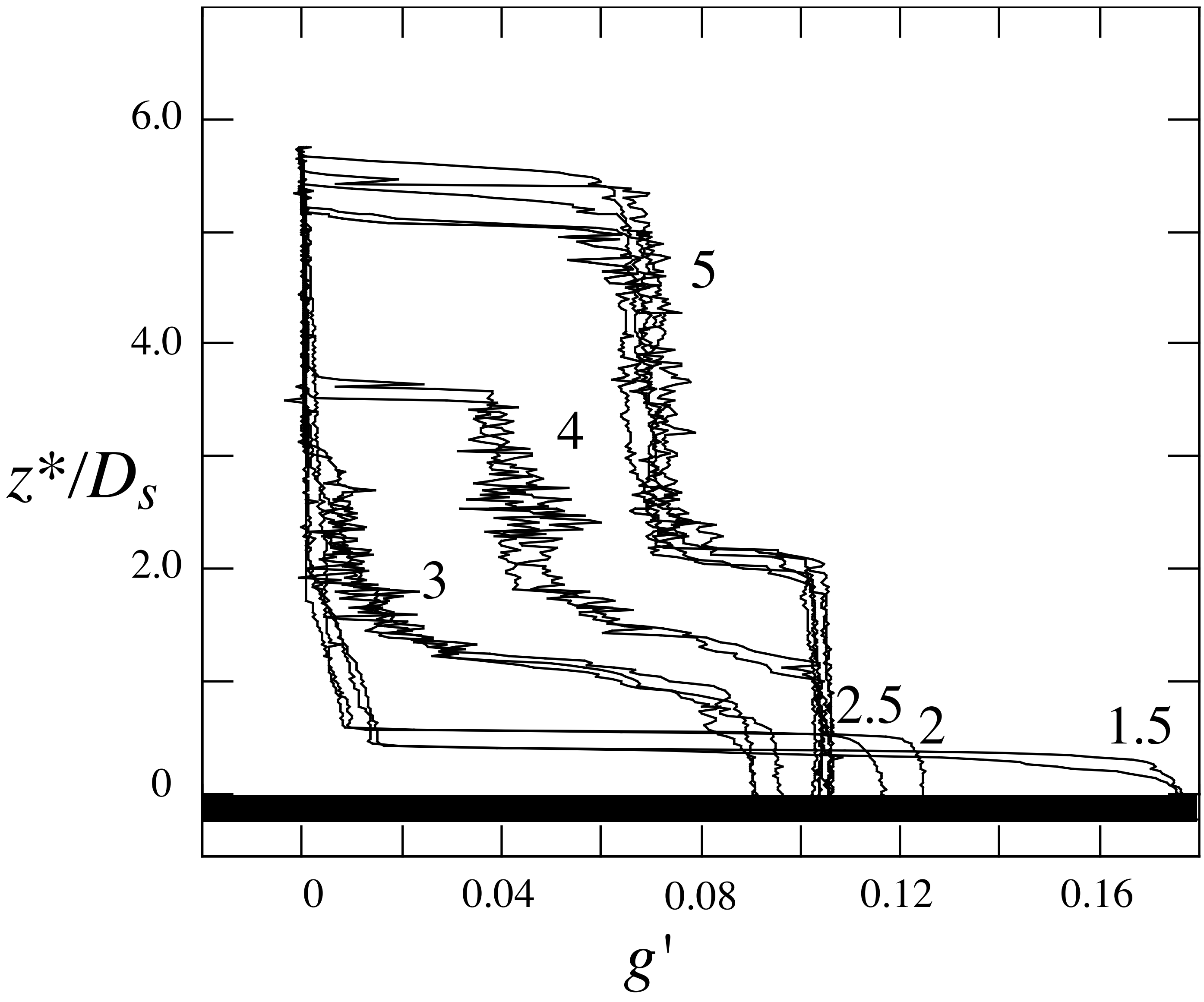

Figure 5.5.7